

Low Driving Voltage, High Quantum Efficiency, High Power Efficiency, and Little Efficiency Roll-Off in Red, Green, and Deep-Blue Phosphorescent Organic Light-Emitting Diodes Using a High-Triplet-Energy Hole Transport Material

Yong Joo Cho and Jun Yeob Lee*

Phosphorescent organic light-emitting diodes (PHOLEDs) have been developed because of high quantum efficiency of phosphorescent emitting materials.^[1–3] A theoretical quantum efficiency over 20% has already been obtained in red, green, and blue colors by synthesizing new emitting materials and charge-transport materials in combination with optimized device architecture.^[4–8]

Many research focused on developing host and dopant materials, but the development of charge transport materials is also important to maximize the light-emitting properties of the phosphorescent emitting materials. There are several requirements for the charge transport materials for PHOLEDs, which include high triplet energy for triplet exciton blocking, highest occupied molecular orbital (HOMO) or lowest unoccupied molecular orbital (LUMO) levels for efficient hole or electron injection, a charge confining HOMO or LUMO level, and high carrier mobility. In particular, a high triplet energy over 2.80 eV is required for the charge-transport materials for deep-blue PHOLEDs because the triplet energy of the deep-blue emitter is around 2.75 eV.^[8,9] Several hole and electron transport materials have been reported as high-triplet-energy charge-transport materials. Typically, carbazole- or diphenylamine-type high-triplet-energy hole transport materials have been used as the hole transport materials for PHOLEDs,^[10–12] while pyridine- or phosphine-oxide-type high-triplet-energy electron transport materials have been widely used.^[13–18] Recently, a diphenylphosphine-oxide-type electron transport material was found to be effective as the high-triplet-energy electron transport layer.^[8]

In the case of the hole transport layer, *N,N'*-dicarbazolyl-3,5-benzene (mCP) was universally used as the high-triplet-energy hole transport material in PHOLEDs.^[19,20] It has a high triplet energy of 2.90 eV for all red, green, and blue applications and moderate hole transport properties in addition to the HOMO level suitable for hole injection into the host material in the emitting layer. However, the mCP suffers from poor thermal stability and high driving voltage. Although 1,1-bis[(di-4-tolylamino)phenyl]cyclohexane (TAPC) shows high triplet energy and high hole mobility, the HOMO level of 5.5 eV is not suitable for hole injection into the emitting layer.^[7] Therefore,

a new hole transport material with a high triplet energy over 2.90 eV, thermal stability, high hole mobility, and HOMO level for efficient hole injection is required.

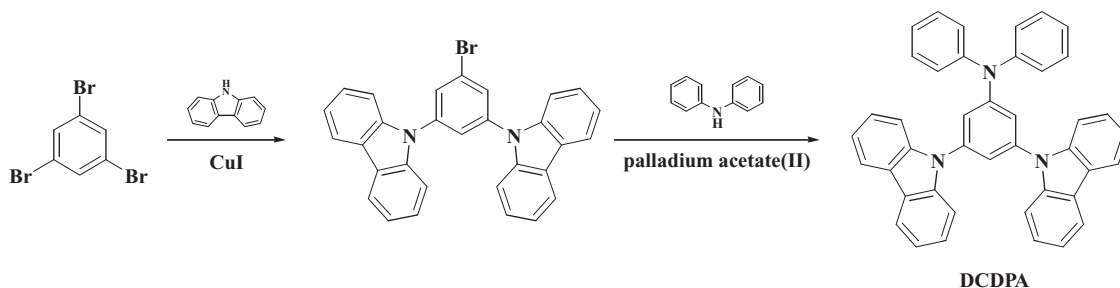
In this work, a new high triplet energy hole transport material, 3,5-di(9H-carbazol-9-yl)-*N,N*-diphenylaniline (DCDPA), was synthesized as the universal hole transport material for red, green, and deep-blue PHOLEDs. It was compared with common mCP in terms of material properties and device performances. It was demonstrated that the DCDPA improved the driving voltage, power efficiency, quantum efficiency and efficiency roll-off of red, green, and deep-blue PHOLEDs while overcoming the poor thermal stability of mCP.

The DCDPA was designed to improve the glass transition temperature (T_g) and hole transport properties of the common mCP while keeping the high triplet energy of mCP. A diphenylamine group was introduced in the molecular structure to improve the hole transport properties of mCP. It has been known that the diphenylamine group is better than the carbazole group in terms of hole transport properties due to strong electron donating property of the diphenylamine group.^[21,22] The introduction of the diphenylamine group can also enhance the T_g of mCP because of the increased molecular rigidity and molecular weight. In addition, the HOMO level of the mCP can be shifted upward to the vacuum level for efficient hole injection and the high triplet energy of the mCP can be maintained because the diphenylamine was introduced at meta position of the carbazole. The meta-substitution can minimize the extension of the conjugation length and the triplet energy of mCP can be maintained. The DCDPA was synthesized by reaction of 1,3,5-tribromobenzene with two equivalents 9H-carbazole followed by reaction with diphenylamine. Synthetic method for the DCDPA is shown in **Scheme 1**. The DCDPA was purified by recrystallization and column chromatography, yielding pure DCDPA powder with a high purity of over 99.0% from high-performance chromatography analysis.

The thermal properties of the DCDPA were measured by differential scanning calorimetry and the T_g of the DCDPA was observed to be 109 °C. The T_g of DCDPA was increased by more than 40 °C compared with that of mCP because of the diphenylamine unit. The additional diphenylamine unit hindered the motion of the molecule, leading to higher T_g in DCDPA than in mCP. The high T_g of the DCDPA improved the high-temperature morphological stability of the DCDPA. The vacuum-deposited mCP film was crystallized even at 70 °C, but the DCDPA film morphology was stable up to 100 °C. The additional diphenylamine group improved the morphological stability at high temperature.

Y. J. Cho, Prof. J. Y. Lee
Department of Polymer Science and Engineering
Dankook University 126
Jukjeon-dong, Suji-gu, Yongin, Gyeonggi, 448-701, Korea
E-mail: leej17@dankook.ac.kr

DOI: 10.1002/adma.201102045



Scheme 1. Synthetic scheme of DCDPA.

Photophysical properties of the DCDPA were analyzed using UV-vis and photoluminescence (PL) measurements. **Figure 1** shows the UV-vis, solution PL, and low temperature PL spectra of the DCDPA. The DCDPA showed the absorption of the carbazole and diphenylamine units at 292 nm, 322 nm, and 338 nm. The bandgap was calculated from the absorption edge of the UV-vis spectra and was 3.54 eV. Compared with the mCP with a bandgap of 3.60 eV (Figure 1a), the bandgap was reduced in the DCDPA because of the diphenylamine unit in the molecular structure. This result agrees with the trend of a simulated bandgap of mCP and DCDPA. The simulated bandgap of DCDPA was 4.48 eV compared with 4.64 eV of mCP. The simulated bandgap was larger than the experimental bandgap. The solution PL measurement was carried out in tetrahydrofuran and PL emission peak was observed at 380 nm. Low temperature PL measurement was performed to measure the triplet energy of the DCDPA hole transport material and the triplet energy was 2.90 eV. The triplet energy of the DCDPA was high enough for triplet exciton blocking in red, green, and deep-blue PHOLEDs. In general, the triplet energy of the deep-blue phosphorescent emitter is between 2.70 eV and 2.75 eV.^[8] Therefore, the DCDPA can effectively suppress the triplet exciton quenching of red, green, and deep-blue emitters by the hole transport layer.

The HOMO level of the DCDPA was measured using cyclic voltametry (Figure S1, Supporting Information) and the LUMO was calculated from the HOMO and bandgap obtained from UV-vis spectrum. The HOMO level of the DCDPA was 5.88 eV from the onset of the oxidation peak and the LUMO level was 2.34 eV. The HOMO level of DCDPA was shifted by 0.22 eV compared with 6.1 eV of the mCP^[23] (5.90 eV by surface

analyzer)^[24] by the strong electron-donating diphenylamine unit. The HOMO level of DCDPA was suitable for hole injection into the host material with the HOMO level range from 5.9 eV to 6.2 eV. The LUMO level was 2.34 eV, which was suitable for electron blocking from the emitting layer. The LUMO level of the DCDPA was more suitable for electron blocking than that of the mCP (2.50 eV). Therefore, the DCDPA can be effective as the hole transport material for PHOLEDs because of HOMO level for good hole injection, the LUMO level for electron blocking, and the high triplet energy for exciton blocking. The shift of the HOMO and LUMO level of the DCDPA compared with those of mCP can be explained by the molecular orbital distribution of DCDPA in Figure 1. Density functional theory calculations for DCDPA were carried out using a suite of the Gaussian 09 computer program^[25] to study the orbital distribution of the DCDPA hole transport material. The nonlocal density functional of Becke's 3-parameters employing Lee–Yang–Parr functional (B3LYP) with 6-31G* basis sets were used for the calculation. The HOMO was localized on the diphenylamine group and carbazole, while the LUMO was localized on the phenyl group attached to the diphenylamine group. The diphenylamine group affected the HOMO and LUMO distribution of DCDPA, shifting the energy levels close to the vacuum level due to strong electron donating properties of the aromatic amine group.

The hole transport properties of DCDPA were compared with those of mCP by fabricating hole-only devices. Hole-only device data for DCDPA and mCP are shown in **Figure 2**. The device structure of hole-only device was indium tin oxide (ITO; 50 nm)/N,N'-diphenyl-N,N'-bis-[4-(phenyl-m-tolyl-amino)-phenyl]-biphenyl-4,4'-diamine (DNTPD, 60 nm)/N,N'-di(1-naphthyl)-N,N'-diphenylbenzidine(NPB, 5 nm)/mCP or DCDPA

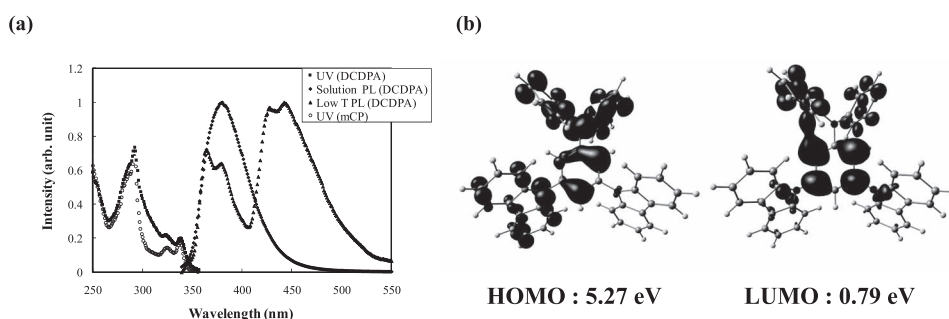


Figure 1. UV-vis absorption and PL spectra (a) of DCDPA and molecular orbital simulation results (b) for DCDPA.

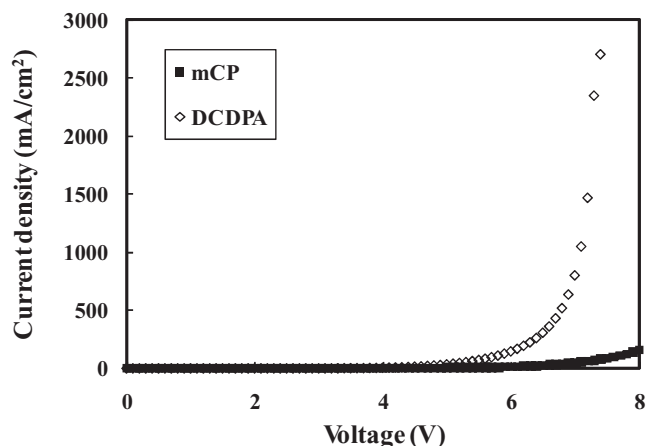


Figure 2. Hole current density of hole-only devices of mCP and DCDPA.

(30 nm)/Al (100 nm). The hole current density of the DCDPA was much higher than that of the mCP over the entire voltage range. The hole current density is generally determined by the energy barrier for hole injection and hole transport properties.

The DCDPA is better than mCP in terms of both hole injection and hole transport. The HOMO level of DCDPA is more suitable for hole injection than that of mCP due to low energy barrier for hole injection from the hole injection layer to the DCDPA in the hole-only device. The hole transport properties are also improved in the DCDPA because of the diphenylamine unit, which has strong electron donating character. Therefore, the DCDPA showed high hole current density and can improve the driving voltage and power efficiency of PHOLEDs

Red, green, and deep-blue PHOLEDs were fabricated to compare DCDPA and mCP as the exciton blocking hole transport materials. An iridium(III) bis-(2-phenylquinoline) acetylacetonate (Ir(pq)₂acac) doped 9,9'-spiro[fluorene]-2-yl(9,9'-spiro[fluorene]-7-yl)methanone (BSFM) layer was used as the red-emitting layer, while iridium(III) tris(2-phenylpyridine) (Ir(ppy)₃)-doped BSFM was used as the green-emitting layer. Deep-blue-emitting layer was iridium(III) bis((3,5-difluoro-4-cyanophenyl)pyridine) picolinate (FCNIpic)-doped 9-(3-(9H-carbazole-9-yl)phenyl-3,6-bis(diphenylphosphoryl)-9H-carbazole (CPBDC). The energy level diagram and triplet energy of the materials are shown in Figure S2 (Supporting Information). All HOMO levels were measured by cyclic voltametry. Figure 3

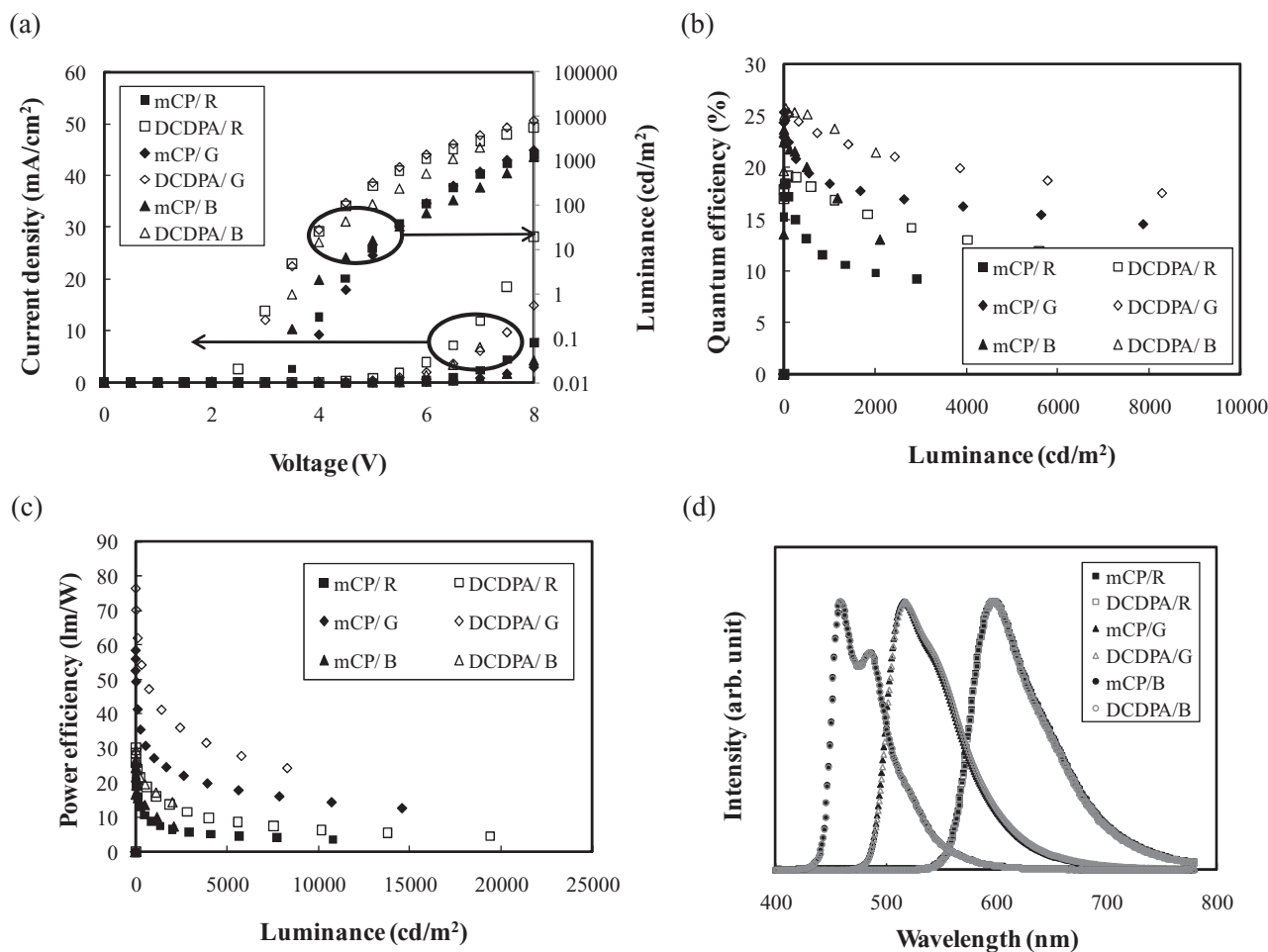


Figure 3. Current density–voltage–luminance (a), quantum efficiency–luminance (b), power efficiency–luminance (c), and electroluminescence (d) data for the red, green, and deep-blue PHOLEDs with DCDPA.

Table 1. Device performances of DCDPA and mCP devices.

	Driving voltage ^{a)} [V]	Maximum quantum efficiency [%]	Quantum efficiency ^{a)} [%]	Power efficiency ^{a)} [lm W ⁻¹]
Red-DCDPA	5.9	19.2	17.1	16.4
Red-mCP	7.7	18.5	11.3	8.3
Green-DCDPA	5.7	25.3	22.9	44.5
Green-mCP	7.4	25.3	18.4	27.3
Blue-DCDPA	6.9	25.8	24.2	17.8
Blue-mCP	8.9	23.6	17.8	10.8

^{a)}Data measured at 1000 cd m⁻².

shows the current density–voltage and luminance–voltage curves of the red, green, and blue PHOLEDs. The current density of the red, green, and deep-blue PHOLEDs was greatly improved by using DCDPA instead of mCP and the driving voltage at the same current density was reduced by about 2.0 V. The significant increase of the current density is caused by the high hole current density, as shown in Figure 2. The increased hole current density contributed to the improvement of the driving voltage at the same current density. Although the energy barrier for hole injection between the DCDPA and the emitting layer was higher than that between the mCP and emitting layer, the good hole transport properties and the low energy barrier for hole injection between the hole injection layer and DCDPA increased the current density of the DCDPA devices. The luminance was also greatly increased by using the DCDPA. The driving voltage at 1000 cd m⁻² was reduced by ≈1.5 V to 2.0 V depending on the color. The driving voltage of the red PHOLED was reduced from 7.7 V to 5.9 V and that of the green PHOLED was lowered from 7.4 V to 5.7 V. The driving voltage of deep-blue PHOLED was changed from 8.9 V to 6.9 V. Therefore, the driving voltage was considerably improved by the DCDPA hole-transport-type exciton blocking layer.

The quantum efficiency–luminance and power efficiency–luminance curves of the red, green, and blue PHOLEDs are also shown in Figure 3. The maximum quantum efficiencies of the red, green, and blue PHOLEDs with mCP hole-transport-type exciton blocking layer were 18.5%, 25.3%, and 23.6%, respectively. The maximum quantum efficiencies of the red, green, and blue PHOLEDs were similar, irrespective of the hole transport material (Table 1). However, the quantum efficiency at 1000 cd m⁻² was greatly enhanced by using the DCDPA instead of mCP. The quantum efficiencies of mCP devices at 1000 cd m⁻² were 11.3%, 18.4%, and 17.8% for red, green, and blue PHOLEDs, while those of DCDPA devices were 17.1%, 22.9%, and 24.2% under the same conditions. Therefore, the quantum efficiency at high luminance was improved by the DCDPA hole transport layer. The efficiency roll-off of the DCDPA device was less than 10% up to 1000 cd m⁻² compared with about 30% for the mCP device. The reduced efficiency roll-off can be explained by the efficient hole transport properties of the DCDPA hole transport material. The efficiency roll-off is induced by the unbalanced charge density at high driving voltage. The degree of increase of electron density is higher than that of hole density at high voltage because of electron transport properties of the host

materials and poor hole transport properties of mCP. However, the efficient hole transport properties of the DCDPA can increase the hole density at high voltage, balancing holes and electrons at high voltage and luminance. Therefore, the efficiency roll-off was suppressed in the DCDPA device. In addition, the triplet energy of the DCDPA was 2.90 eV, which was high enough for triplet exciton blocking in the red, green, and deep-blue PHOLEDs, resulting in high quantum efficiency in the DCDPA-based PHOLEDs. The LUMO level of 2.34 eV of DCDPA also contributed to the high quantum efficiency by electron blocking effect. The energy barrier for electron blocking was high in DCDPA device compared with mCP device. There was at least 0.21 eV energy barrier for electron injection from the host to the DCDPA layer (Figure S2, Supporting Information), which blocked the electron leakage to the hole transport layer.

The power efficiency of DCDPA device was also improved by the DCDPA device. The power efficiencies of the DCDPA devices at 1000 cd m⁻² were 16.4 lm W⁻¹, 44.5 lm W⁻¹, and 17.8 lm W⁻¹ compared with 8.3 lm W⁻¹, 27.3 lm W⁻¹, and 10.8 lm W⁻¹ of mCP for red, green, and blue PHOLEDs. The power efficiency was doubled in red PHOLEDs and was enhanced by more than 70% in green and blue PHOLEDs. The improved power efficiency of the DCDPA device originates from the low driving voltage and high quantum efficiency. As explained above, the lowered driving voltage and increased quantum efficiency of the DCDPA device induced the improvement of the power efficiency.

In conclusion, a novel high-triplet-energy hole transport material, DCDPA, was effective to improve the driving voltage, quantum efficiency at high luminance, power efficiency, and efficiency roll-off of red, green, and deep-blue PHOLEDs. The DCDPA could be universally used as the hole-transport-type exciton-blocking layer in all red, green, and deep-blue PHOLEDs because of the high triplet energy, good hole injection properties, and electron blocking properties. This approach can be useful for further development of high-triplet-energy hole transport materials for red, green, and deep-blue PHOLEDs.

Experimental Section

Synthesis: Detailed synthetic procedure and general analysis of the material are described in the Supporting Information.

Device Fabrication and Measurements: The basic device structure of PHOLEDs was ITO (50 nm)/DNTPD (60 nm)/NPB (5 nm) or poly(3,4-eth

ylenedioxythiophene):polystyrenesulfonate (PEDOT:PSS) (60 nm)/mCP or DCDPA (30 nm)/host:dopant (30 nm, 3%)/diphenylphosphine oxide-4-(triphenylsilyl)phenyl (25 nm)/LiF (1 nm)/Al (200 nm). DNTPD/NPB was the hole injection layer for red and green devices, while PEDOT:PSS was the hole injection layer for blue devices. The red-emitting material was Ir(pq)₂acac-doped BSFM, while the green-emitting material was Ir(ppy)₃-doped BSFM. FCNIrpic-doped CPBDC was the blue-emitting material. All devices were encapsulated with a glass lid and a CaO getter after device fabrication. Hole-only devices with a device structure of ITO/DNTPD/NPB/mCP or DCDPA/Au were fabricated to compare hole current density of mCP and DCDPA. The device performances of the red, green, and blue PHOLEDs were measured with a Keithley 2400 source measurement unit and CS1000 spectroradiometer after encapsulation.

Supporting Information

Supporting Information is available from the Wiley Online Library or from the author.

Received: June 1, 2011

Revised: August 10, 2011

Published online: September 8, 2011

- [1] M. A. Baldo, D. F. O'Brian., Y. You, A. Shoustikov, S. Sibley, M. E. Thompson, S. R. Forrest, *Nature* **1998**, 395, 151.
- [2] M. A. Baldo, D. F. O'Brian, M. E. Thompson, S. R. Forrest, *Phys. Rev. B* **1999**, 60, 14422.
- [3] D. F. O'Brien, M. A. Baldo, M. E. Thompson, S. R. Forrest, *Appl. Phys. Lett.* **1999**, 74, 442.
- [4] C. Adachi, M. A. Baldo, M. E. Thompson, S. R. Forrest, *J. Appl. Phys.* **2001**, 90, 5048.
- [5] S.-J. Su, D. Tanaka, Y.-J. Li, H. Sasabe, T. Takeda, J. Kido, *Org. Lett.* **2008**, 10, 941.
- [6] L. Xiao, S.-J. Su, Y. Agata, H. Lan, J. Kido, *Adv. Mater.* **2009**, 21, 1271.
- [7] N. Chopra, J. Lee, Y. Zheng, S.-H. Eom, J. Xue, F. So, *Appl. Phys. Lett.* **2008**, 93143307.
- [8] S. O. Jeon, S. E. Jang, H. S. Son, J. Y. Lee, *Adv. Mater.* **2011**, 23, 1436.
- [9] H. Sasabe, J. Takamatsu, T. Motoyama, S. Watanabe, G. Wagenblast, N. Langer, O. Molt, E. Fuchs, C. Lennartz, J. Kido, *Adv. Mater.* **2010**, 22, 5003.
- [10] S. O. Jeon, K. S. Yook, C. W. Joo, J. Y. Lee, *Adv. Mater.* **2010**, 22, 1872.
- [11] S. O. Jeon, K. S. Yook, C. W. Joo, J. Y. Lee, *Adv. Funct. Mater.* **2009**, 19, 3644.
- [12] M.-T. Lee, J.-S. Lin, M.-T. Chu, M.-R. Tseng, *Appl. Phys. Lett.* **2009**, 94, 083506.
- [13] S. Su, E. Gonmori, H. Sasabe, J. Kido, *Adv. Mater.* **2008**, 20, 4189.
- [14] H. Sasabe, E. Gonmori, T. Chiba, Y.-J. Li, D. Tanaka, S.-J. Su, T. Takeda, Y.-J. Pu, K. Nakayama, J. Kido, *Chem. Mater.* **2008**, 20, 5951.
- [15] P. A. Vecchi, A. B. Padmaperuma, H. Qiao, L. S. Sapochak, P. E. Burrows, *Org. Lett.* **2006**, 8, 4211.
- [16] X. Cai, A. B. Padmaperuma, L. S. Sapochak, P. A. Vecchi, P. E. Burrows, *Appl. Phys. Lett.* **2008**, 92, 083308.
- [17] D. Kim, S. Salman, V. Coropceanu, E. Salomon, A. B. Padmaperuma, L. S. Sapochak, A. Kahn, J.-L. Bredas, *Chem. Mater.* **2010**, 22, 247.
- [18] S. Kwon, K.-R. Wee, A.-L. Kim, S. O. Kang, *J. Phys. Chem. Lett.* **2010**, 1, 295.
- [19] R. J. Holmes, B. W. D'Andrade, S. R. Forrest, X. Ren, J. Li, M. E. Thompson, *Appl. Phys. Lett.* **2003**, 83, 3818.
- [20] K. Goushi, R. Kwong, J. J. Brown, H. Sasabe, C. Adachi, *J. Appl. Phys.* **2004**, 95, 7798.
- [21] L. S. Hung, C. H. Chen, *Mater. Sci. Eng.* **2002**, 39, 143.
- [22] Q. Zhang, J. Chen, Y. Cheng, L. Wang, D. Ma, X. Jing, F. Wang, *J. Mater. Chem.* **2004**, 14, 895.
- [23] J. Jou, W. Wang, S. Chen, J. Shyue, M. Hsu, C. Lin, S. Shen, C. Wang, C. Liu, C. Chen, M. Wu, S. Liu, *J. Mater. Chem.* **2010**, 20, 8411.
- [24] V. Adamovich, J. Brooks, A. Tamayo, A. M. Alexander, P. I. Djurovich, B. W. D'Andrade, C. Adachi, S. R. Forrest, M. E. Thompson, *New J. Chem.* **2002**, 26, 1171.
- [25] M. J. Frisch, G. W. Trucks, H. B. Schlegel, G. E. Scuseria, M. A. Robb, J. R. Cheeseman, J. A. Montgomery, T. Vreven, Jr., K. N. Kudin, J. C. Burant, J. M. Millam, S. S. Iyengar, J. Tomasi, V. Barone, B. Mennucci, M. Cossi, G. Scalmani, N. Rega, G. A. Petersson, H. Nakatsuji, M. Hada, M. Ehara, K. Toyota, R. Fukuda, J. Hasegawa, M. Ishida, T. Nakajima, Y. Honda, O. Kitao, H. Nakai, M. Klene, X. Li, J. E. Knox, H. P. Hratchian, J. B. Cross, C. Adamo, J. Jaramillo, R. Gomperts, R. E. Stratmann, O. Yazyev, A. J. Austin, R. Cammi, C. Pomelli, J. W. Ochterski, P. Y. Ayala, K. Morokuma, G. A. Voth, P. Salvador, J. J. Dannenberg, V. G. Zakrzewski, S. Dapprich, A. D. Daniels, M. C. Strain, O. Farkas, D. K. Malick, A. D. Rabuck, K. Raghavachari, J. B. Foresman, J. V. Ortiz, Q. Cui, A. G. Baboul, S. Clifford, J. Cioslowski, B. B. Stefanov, G. Liu, A. Liashenko, P. Piskorz, I. Komaromi, R. L. Martin, D. J. Fox, T. Keith, M. A. Al-Laham, C. Y. Peng, A. Nanayakkara, M. Challacombe, P. M. W. Gill, B. Johnson, W. Chen, M. W. Wong, C. Gonzalez, J. A. Pople, *Gaussian 03*, revision B05, Gaussian, Inc: Pittsburgh, PA, **2003**.